International Journal of Biological Macromolecules 237 (2023) 123955

Contents lists available at ScienceDirect

International Journal of Biological Macromolecules

journal homepage: www.elsevier.com/locate/ijbiomac

Coating with cationic inulin enhances the drug release profile and *in vitro* anticancer activity of lecithin-based nano drug delivery systems

Ozgun Vatansever [a], Fatemeh Bahadori [b,c], Seyma Bulut [d,e], Mehmet Sayip Eroglu [f,g,*]

[a] Department of Chemical Engineering, Marmara University, Aydınevler, Maltepe, 34854, Istanbul, Turkey
[b] Department of Pharmaceutical Biotechnology, Faculty of Pharmacy, BezmialemVakif University, 34093 Istanbul, Turkey
[c] Department of Analytical Chemistry, Faculty of Pharmacy, Istanbul University-Cerrahpasa, Buyukcekmece Campus, 34500 Istanbul, Turkey
[d] Department of Biotechnology, Institute of Health Sciences, Bezmialem Vakif University, 34093 Fatih, Istanbul, Turkey
[e] Department of Medical Biophysics, Faculty of Medicine, BezmialemVakif University, 34093 Istanbul, Turkey
[f] Department of Materials Science and Engineering, Technology Faculty, Marmara University, Aydınevler, Maltepe 34854, Istanbul, Turkey
[g] TUBITAK-UME, Chemistry Group Laboratories, PO Box 74, 41470 Gebze, Kocaeli, Turkey

ARTICLE INFO

Keywords:
Lecithin
Drug delivery systems
Solid lipid nanoparticles
Inulin, drug release kinetics

ABSTRACT

Core-shell structured lipidic nanoparticles (LNPs) were developed using lecithin sodium acetate (Lec-OAc) ionic complex as a core unit and quaternized inulin (QIn) as the shell part. Inulin (In) was modified using glycidyl trimethyl ammonium chloride (GTMAC) as a positively charged shell part and used for coating the negatively surface charged Lec-OAc. The critical micelle concentration (CMC) of the core was determined as 1.047×10^{-4} M, which is expected to provide high stability in blood circulation as a drug-carrying compartment. The amounts of curcumin (Cur) and paclitaxel (Ptx) loaded to LNPs (CurPtx-LNPs), and quaternized inulin-coated LNPs (CurPtx-QIn-LNPs) were optimized to obtain mono-dispersed particles with maximum payload. The total amount of 2.0 mg of the drug mixture (1 mg Cur and 1 mg Ptx) was the optimized quantity for QIn-LNPs and CurPtx-QIn-LNPs due to the favorable physicochemical properties determined by dynamic light scattering (DLS) studies. This inference was confirmed by differential scanning calorimeter (DSC), and Fourier-transform infrared (FT-IR). SEM and TEM images clearly revealed the spherical shapes of LNPs and QIn-LNPs, and QIn covered the LNPs completely. The cumulative release measurements of Cur and Ptx from CurPtx-QIn-LNPs, along with the kinetic studies, showed a significant decrease in the release period of drug molecules with the effect of the coating. At the same time, Korsmeyer-Peppas was the best diffusion-controlled release model. Coating of the LNPs with QIn increased the cell-internalization of NPs to the MDA-MB-231 breast cancer cell lines, resulting in a better toxicity profile than the empty LNPs.

1. Introduction

Curcumin (Cur), a yellow hydrophobic polyphenol compound, is an active ingredient extracted from *Curcuma longa* rhizomes and classified in class IV of the biopharmaceutics due to its poor water solubility and intestinal permeation. It is known for its anti-inflammatory, antimicrobial, antioxidant, anticancer, antidiabetic, antidepressant, anti-Alzheimer, and antitumor characteristics. Furthermore, Cur has been used to treat cancer, cystic fibrosis, malaria, Parkinson's disease, multiple sclerosis, and hypertension. It is known to prevent the development of cancerous cells by induction of cell cycle arrest and apoptosis, which are important through pleiotropic modulation on different cancer targets that include NF-κB, cyclooxygenase-2 (COX-2), tumor necrosis factor-alpha (TNF-α), STAT-3, and cyclin D1 [1]. On the other hand, despite the several advantages of Cur, its poor solubility in aqueous media, instability in living organisms, low tissue absorption, and poor bioavailability have obstructed its clinical and drug applications. To overcome these limitations, Cur and other phenolic anticancer compounds were encapsulated in nano/micro drug delivery systems (NDDS) such as liposomes, polymeric nanoparticles (NPs), hydrogels, *etc.* [2–8].

Paclitaxel (Ptx), one of the most effective chemotherapeutic agents in pharmaceutical history, with a broad range of efficacy on different cancer types, is also a poorly water-soluble compound, which was commercialized in a formulation of Cremophor EL and dehydrated

* Corresponding author at: Department of Materials Science and Engineering, Technology Faculty, Marmara University, Aydınevler, Maltepe, 34854, Istanbul, Turkey.
E-mail address: mehmet.eroglu@marmara.edu.tr (M.S. Eroglu).

https://doi.org/10.1016/j.ijbiomac.2023.123955
Received 7 January 2023; Received in revised form 24 February 2023; Accepted 4 March 2023
Available online 9 March 2023

ethanol (50:50, v/v). These excipients cause considerable side effects, which can be eliminated using NDDS [9]. NDDS can accumulate in cancer tumors by taking advantage of the Enhanced Permeability and Retention (EPR) effect [10]. Furthermore, the distribution of conventional chemotherapeutic agents in the blood circulation system and their elimination by macrophages reduce their accumulation ratio in tumor cells. A lower dose of chemotherapy agents not only reduces the chance of curing but also causes the development of chemo-resistant cancer tumors, which is a widespread obstacle associated with Ptx administration [11]. It has been shown that targeting transcription factor NF-κB is one of the most efficient way to overcome the chemo-resistance [11]. Cur can inhibit transcription factor NF-κB and reduces the chemo-resistance caused by Ptx [12]. However, in order to maximize the inhibition activity of Cur and the efficacy of Ptx, development of their nano-formulations to target tumors using NDDS is crucial.

The most desired properties for drug delivery systems are admissible stability, half-life, and good toxicity profile [13]. Nowadays, lipid nanoparticles (LNPs), which are colloidal drug delivery systems consisting of liposomes and polymeric molecules, have gained much attention. They present better stability than similar solid matrixes, and higher biocompatibility compared to other lipid-based structures.

In this study, Ptx and Cur are encapsulated in a novel NDDS possessing lecithin-acetate (Lec-OAc) core and quaternized inulin (QIn) outer shell. Lecithin, which is a zwitterionic phospholipid molecule, has an amphiphilic character. Although it is used for controlled drug release [5], it has some important drawbacks, such as crystallization and negative surface charges, which hinder the cell-internalization of LNPs on the cancer tumor side. Thus, surface coatings with LNPs are accomplished using a polysaccharide polymer, inulin (In) [14]. It is a linear fructan form of D-fructose, connected through β-(2,1)-glycosidic linkages. Inulin is abundant, and non-toxic material, the safety of which was approved by the FDA [15]. In addition, the antitumor activity of inulin was observed on Lewis pulmonary carcinoma implanted in mice [16].

QIn is a synthetic derivative of In, which was synthesized by the reaction of free hydroxymethyl groups of inulin with epoxide parts of glycidyl trimethyl ammonium chloride (GTMAC). It is a cationic polymer with positive pendant charges that can electrostatically interact with anionic cell surfaces and mucosa. In this study, QIn-coated phospholipid nanoparticles (QIn-LNPs) have been developed for better drug delivery systems, preventing agglomeration and oxidation of LNPs [17,18].

2. Materials and methods

2.1. Materials

Inulin was purchased from Cosucra (Belgium) and used without further purification. Analytical grade dichloromethane (DCM) was obtained from Merck (Germany), and glycidyltrimethylammonium chloride (GTMAC), acetone, pyrene, curcumin, and polyoxyethylene sorbitan monooleate (Tween 80) from Sigma Aldrich. Soybean lecithin powder GPR Rectapur was purchased from VWR Chemicals. Sodium acetate (NaOAc) was obtained from Carlo Erba Reagents. Dialysis tubing Amicon® Ultra-15 Centrifugal Filter Unit, MWCO 3000, was used in release studies and purchased from Merck-Millipore. Ultra-pure water (UPW) was used in all experimental stages. MDA-MB-231 (HTB-26), breast mammary gland adenocarcinoma cells, and all cell culture materials were purchased from ATCC.

2.2. Preparation of lecithin-sodium acetate (Lec-OAc) complex

Lec-OAc (1 mol:1 mol) complex was prepared according to the method described in the literature [19]. Initially, 0.2 M lecithin solution in 15 mL of UPW was prepared at 80 °C under vigorous stirring for 3 h. 0.2 M sodium acetate solution in 15 mL UPW was prepared and added to the 0.2 M lecithin solution at 80 °C to form the Lec-OAc complex. The obtained solution was kept at −60 °C and then lyophilized to establish a cation exchange between lecithin and sodium acetate. The dried complex was extracted at room temperature with DCM and kept in a vacuum oven at 30 °C for 24 h to remove DCM. The formed complex was kept in a refrigerator at 4 °C until use.

2.3. Synthesis of quaternized inulin (QIn)

QIn was synthesized according to the method reported in the literature [20]. 2.0 g of inulin (9.2 mmol of fructose groups) was dissolved in a 75 mL alkaline aqueous solution (2 % NaOH). To this solution, 1.5 mL (11.0 mmol) of GTMAC was added dropwise under vigorous stirring. The mixture was heated to 71 °C with a stirring at 300 rpm for 24 h. The reaction mixture was cooled to room temperature, and added to cold acetone (4 °C) dropwise to precipitate the QIn. The cloudy dispersion was kept in a refrigerator for three days to complete the precipitation and the precipitant was decanted, washed with acetone to remove any remaining impurity and filtered. Finally, the product was vacuum dried at 30 °C for one day, which yielded 2.4 g of QIn as a white solid. The degree of quaternization was determined as 35 % based on fructose units of In using ^{1}H NMR spectroscopy. The synthesis of QIn is outlined in Scheme 1.

2.4. Nuclear magnetic resonance spectroscopy (NMR) characterization

^{1}H NMR spectra of native inulin, quaternized inulin, lecithin, and the Lec-ONa complex were monitored using a Varian 600 MHz NMR. While D_2O was used as a solvent for In, QIn, and lecithin, $CDCl_3$ was used for Lec-OAc complex.

2.5. Preparation of Cur and Ptx loaded Lec-OAc NPs

Optimization of the drug delivery system was conducted in two successive steps. Before loading Ptx, Cur was uploaded to Lec-OAc LNPs, and characterization and optimization of Cur-Lec-OAc were performed. Thus, in a round bottom flask (RBF), 10 mg of Lec-OAc complex was dissolved in 10 mL of DCM and the solution was vortexed. Three Cur samples of 0.5 mg, 1.0 mg, and 2.0 mg were dissolved in 5.0 mL of DCM separately and added into a Lec-OAc-containing RBF, and vortexed. DCM was removed under reduced pressure to obtain a thin film inside RBF. The obtained film was dried in a vacuum oven at room temperature overnight, and 30 mL of deionized water was added and emulsified using a homogenizer (Wisd, Daihan Scientific HG-15D model) at 500 rpm for 15 min. The product Cur-Lec-OAc NPs were lyophilized and kept for further use. The experiment indicated that 2 mg curcumin was the best-fitted drug into the core part of the synthesized drug delivery system, giving the monodispersed particles the best release period. Thus, 0, 5, 1, and 2 mg of Ptx samples dissolved in DCM were uploaded to the NDDS along with Cur so that the total drug load was 2.0 mg. The following steps were conducted by using the same procedure above to obtain Cur and Ptx loaded, and surface-coated LNPs (CurPtx-QIn-LNPs).

2.6. Preparation of quaternized inulin coated LNPs (QIn-Lec-OAc)

10 mg of QIn was vortexed in 1 mL of deionized water. Similarly, Cur-Lec-OAc and Cur-PTX-QIn-LNPs were vortexed in 30 ml of UPW. Then, QIn solutions were added to the Cur-Lec-OAc solutions. Subsequently, the final mixtures were emulsified with a homogenizer. The obtained dispersions were lyophilized and kept in the refrigerator for further use. The preparation method of QIn-coated Cur-Ptx loaded NPs is given in Fig. 1.

2.7. Critical micelle concentration (CMC) of Lec-OAc

Critical micelle concentration is a crucial parameter in developing drug delivery systems and surfactants. Surfactant molecules, also known

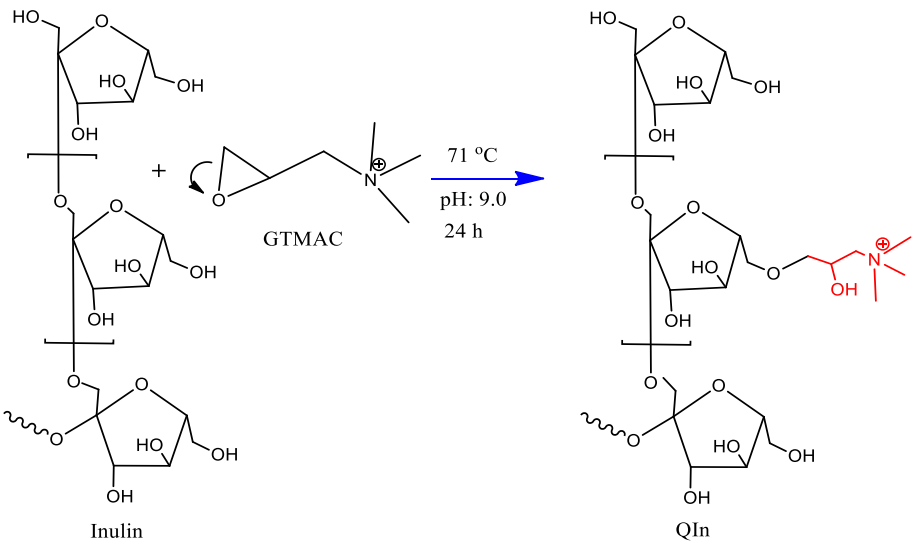

Scheme 1. Synthesis of quaternized inulin (Qin)

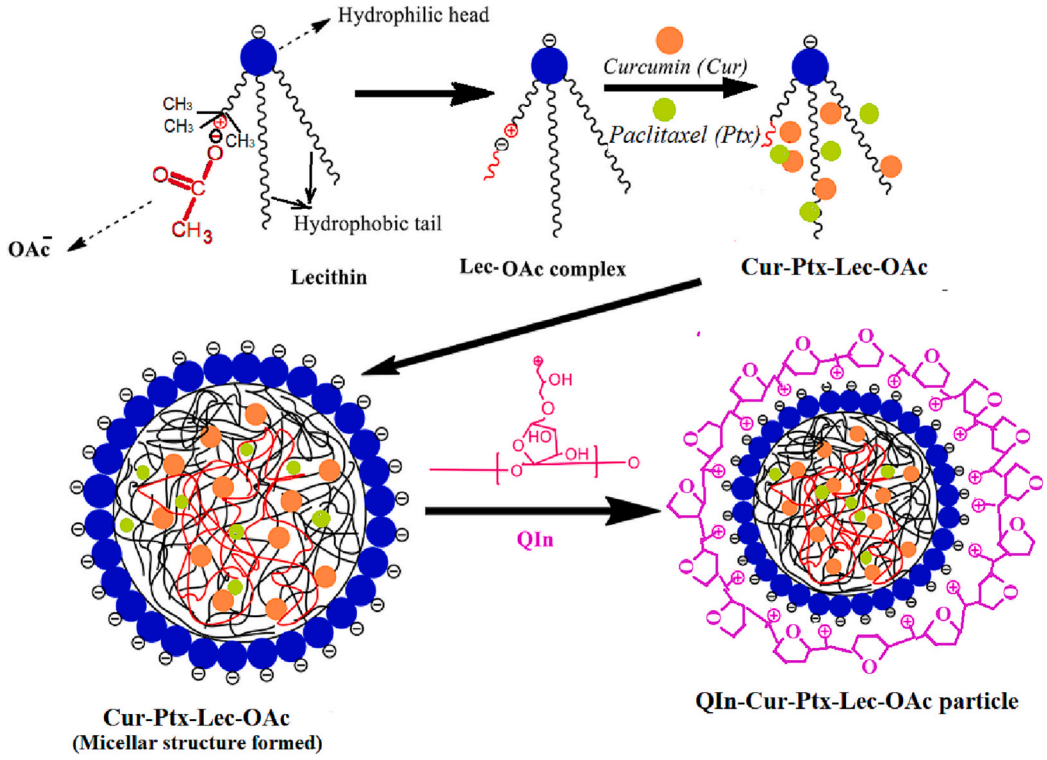

Fig. 1. Preparation method of QIn-coated Cur-Ptx-Lec-OAc NPs.

as surface-active agents, are amphiphilic molecules composed of hydrophobic and hydrophilic pars. When a surfactant molecule is added to an aqueous medium, the surface tension of the solution is reduced due to the alignment of the surfactant molecules at the air-water interface. Once the surface is sufficiently saturated with monomers, the monomers aggregate into spherical clusters called micelles.

The CMC of the core part of NDDS consisting of the Lec-OAc complex was determined by fluorescence spectroscopy in aqueous media using an FS2 model fluorescence spectrophotometer and (Scinco) with a Floro-Master FS-2 software. 6.7×10^{-7} M Pyrene solution in acetone and 9 mM of Lec-OAc complex in 100 mL of UPW were prepared. A thin film of pyrene was obtained by evaporating the solvent acetone. 9 mM Lec-OAc solution was diluted and vortexed with 6.7×10^{-7} M pyrene solution for at least 5 min to obtain different Lec-OAc concentrations (7 mM, 5 mM, 3 mM, 2 mM, 1 mM, 10^{-1} mM, $10^{-1.5}$ mM, 10^{-2} mM, $10^{-2.5}$ mM, 10^{-3} mM, $10^{-3.5}$ mM and 10^{-4} mM). Pyrene-carrying Lec-OAc micelles were incubated at room temperature for an hour, and the steady-state fluorescence spectra were recorded exciting at 343 nm. The peak intensities at 360 nm (I_1) and 386 nm (I_3) were determined. The CMC of the complex was determined as the concentration corresponding to the sharp increase in the I_3/I_1 emission intensity ratio [21].

2.8. The drug release studies of Cur and Cur-Ptx

Regarding the release studies of Cur and Cur-Ptx mixture, QIn-coated NPs carrying a total amount of 2 mg drug were incubated in Millipore-

Amicon® Ultra-15 Centrifugal Filter Unit at 37 °C with a constant shaking at 150 rpm. A solution of 50 % Tween 80 was placed into the basolateral compartment of the dialysis tube, and centrifuged for 5 min at 6000 rpm. The centrifuge was continued at 0.5, 1, 2, 3, 4, 5, 6, 7, 8, 9, 10, and 24 h of incubation. The sample volume at the apical compartment was kept constant by adding UPW after each centrifuge. The amount of Cur in release media was determined using an Elisa reader spectrophotometer at the specific peak intensity of $\lambda_{em} = 520$ nm ($\lambda_{ex} =$ 425 nm), and the amount of Ptx was determined using an HPLC method. Two Hewlett-Packard 1100 (Boeblingen, Germany) HPLC instrument equipped with PDA detector was used. The Supelco type chromatography column (Taufkirchen, Germany) Supelcosil LC-F (stationary phase: pentafluorophenyl), 5 μm, 25 cm × 4.6 mm with column temperature at 25 °C was used. The detection was achieved at $\lambda = 227 \pm 2$ nm. The mobile phase consisted of water and acetonitrile in a gradient elution according to the following program; (i) from start to 18 min, 40 % acetonitrile; (ii) from 18 to 20 min, 45 % acetonitrile; and (iii) from 20 to 35 min, 100 % acetonitrile. The injection volume was 10 μL, and the mobile phase flow rate was kept constant at 1 mL min^{-1}. The drug release ratio was plotted as a function of time [22].

2.9. Particle size and zeta potential measurements

Particle size distribution and zeta potential values of QIn-coated and uncoated LNPs were determined at 25 °C using Zetasizer Nano-ZSP (Malvern Instruments). Before the measurements, the solutions of the NPs were kept at room temperature for 20 min. The measurements were performed using ordinary disposable cuvettes and zeta cuvettes.

2.10. Differential scanning calorimetry (DSC)

Lec-OAc complexes, drug-loaded NPs, and QIn-coated NPs were characterized using Perkin Elmer Jade DSC at a heating range of 10 °C/min under an argon atmosphere (200 ml/min). The samples were heated from 30 °C to 290 °C. DSC thermograms were recorded and evaluated using Pyris software.

2.11. Fourier transform infrared spectroscopy (FT-IR) characterizations

FT-IR spectra of soy lecithin, Lec-OAc, In, and QIn were recorded using Thermo Nicolet 6700 FT-IR spectrophotometer between 400 and 4000 cm^{-1}. The obtained data were collected and evaluated using OMNIC software.

2.12. SEM and TEM

Scanning electron microscopy (SEM) images of the samples were obtained using HITACHI SU 5000 FEG-SEM-TEM&EDS having Schottky Gun and DEBEN-TEM detector. Before recording the SEM images, creamy lyophilized samples were applied on a conductive carbon ribbon and left for 30 min at room temperature. Then, SEM images were obtained under high vacuum mode with an acceleration voltage of 25 kV at 50 K and 90 K magnifications. Transmission electron microscopy (TEM) images were obtained using HITACHI HT7800 model TEM instrument with an acceleration voltage of 100 kV at 60 K and 100 K magnifications.

2.13. In vitro cytotoxicity assay

The cytotoxicity of empty QIn-LNP and CurPtx-QIn-LNP was studied on the breast cancer cell line MDA-MB-231 *in vitro*. The MTT assay was used to study the cell death mechanism. MDA-MB-231 cells were seeded to 96 well plates at 1×10^4 cells/well density. Cur and Ptx were dissolved in 0.1 % DMSO and used as control. Each formulation (10 μL) was added to the 90 μL of media. After diluting the formulations, the same concentrations of controls were used. Empty NDDS (QIn-LNP) at its highest tested concentration was applied in the same volume to study the toxicology of NPs without carrying drugs. After 24, 48, and 72 h of incubations, the cell death mechanism was investigated using MTT assay (Sigma, USA). Briefly, 5 mg/mL MTT solution was added to the culture plates to a final concentration of 0.5 mg/mL. The plates were incubated for 3.5 h at 37 °C, and the formazan residue was then dissolved in 200 μL of DMSO. The absorbance was recorded at 490 nm (Elisa reader (Synergy-H1)).

2.14. Statistical analysis

Cell viability outcomes were evaluated statistically, and the final results were expressed as Mean ± SD. The results are presented as three replicates. Data in the experiments were analyzed using analyses of variance (One-Way ANOVA). Efficacy comparison was made between the cytotoxic efficacy of Cur-Ptx-QIn-LNPs, and other groups (bare Cur, Ptx, CurPtx-LNPs) were analyzed using the one-way analysis of variance. The p-value < 0.05 was considered statistically significant. The comparison between other groups was not carried out since it was out of the aim of the research and to keep the results understandable. All statistical analyzes were done by using the SPSS package program for Windows (Version 11.5).

3. Results and discussion

3.1. NMR of inulin and quaternized inulin

Quaternized inulin was synthesized through the reaction of inulin with glycidyltrimethylammonium chloride (GTMAC) in basic medium. In ^{1}H NMR spectrum of native In (Fig. 2A), hydrogen peaks of fructose rings at (ppm) H1(3.57, 3.73), H3(4.12), H4 (3.97), H5(3.79) and H6 (3.64, 3.71). In the NMR spectrum of QIn (Fig. 2B), new peaks appeared at (ppm) H7(4.31), H9(3.38), H11(3.11) are due to the GTMAC. The degree of quaternization was calculated to be 35 % from the integration of the peaks of H8 at 3.11 ppm, corresponding to methyl groups of the quaternary ammonium salt (–$N(CH_3)_3$), and the fructose H3 peak at 4.13 ppm (Fig. 2B). This evidenced the quaternization of inulin with GTMAC [23].

3.2. NMR of soy-lecithin and Lec-OAc ionic complex

^{1}H NMR spectra of soy-lecithin and Lec-OAc complex in $CDCl_3$ are given in Fig. 3A and B, respectively. In the ^{1}H NMR spectrum of Soy-Lec, the characteristic chemical proton shifts were determined at (ppm) 0.90 (–CH_3), 1.25 (–CH_2), 1.58 (CH_2), 2.1 (CH_2-C═), 2.30 (C═O-CH_2–), 3.30 (N-CH_3) [trimethyl ammonium] and 5.3 (–CH═CH–) [24–28] (Fig. 3A).

Regarding ^{1}H NMR spectrum of the Lec-OAc complex in $CDCl_3$ (Fig. 3B), a characteristic acetate methyl proton peak of OAc at 1.92 ppm was observed, which was reported to be at between 2.4 and 1.92 ppm in the literature [29,30]. Thus, the presence of required NMR peaks along with the presence of acetate methyl peak and insolubility of OAc^- in DCM, Lec-OAc complex was considered to be formed through the cation exchange reaction. This result was confirmed by the integration of the peaks at 0.90 ppm (-CH_3 groups of lecithin) and 1.92 ppm (–CH_3 group of OAc^-) as well.

3.3. The FT-IR characterization of soy lecithin, Lec-OAc, In, and QIn

FT-IR is an easy and fast technique to detect structural transformations occurred in a reaction. Therefore, formation of the Lec-OAc ionic complex was also analyzed by FT-IR (Fig. 4). In FT-IR spectrum of soy lecithin, a broad absorption peak between 3200 and 3600 cm^{-1} is due to the –OH stretching peak of absorbed water. The strong absorption bands at 2921 cm^{-1} and 2852 cm^{-1} are from the CH_2 asymmetric and symmetric stretching modes, respectively. A band at 1376 cm^{-1} was assigned to the symmetric bending absorption of $(CH_3)_3N^+$ groups. A strong characteristic peak at 1735 cm^{-1} is due to the carbonyl stretching

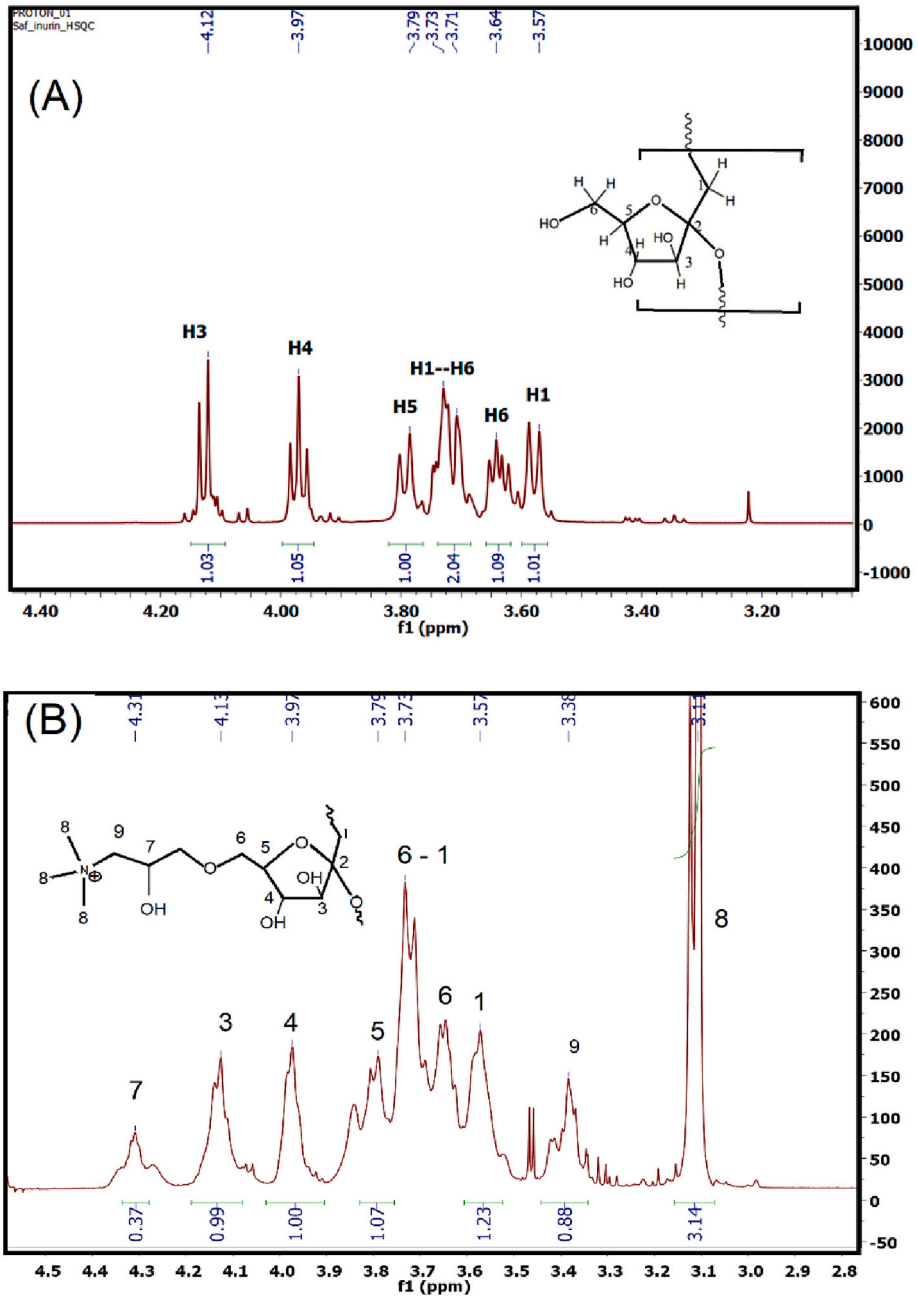

Fig. 2. ^{1}H NMR spectra of inulin (A); quaternized inulin (B).

band (–C═O—O–) of ester groups. The etheric CO—O—C and C—O—P symmetric stretching absorption peaks of lecithin were observed at 1070 cm^{-1} and 1047 cm^{-1}, respectively. In the FT-IR spectrum of Lec-OAc complex, in addition to the characteristic peaks of lecithin, the carbonyl stretching band of acetate groups (–C═O—O–) appeared at 1561 cm^{-1}, which was good indication of the formation of the Lec-OAc ionic complex. As the complex was formed in water, it was removed by lyophilization and the Lec-OAc ionic complex was extracted with dichlorometane (DCM). Considering the insolubility of OAc in DCM, the presence of characteristic acetate and lecithin peaks at the FT-IR spectrum was considered to be evidence for the formation of stable Lec-OAc complex. [31–40].

3.4. Critical micelle concentration (CMC) of Lec-OAc

Critical micelle concentration (CMC) is an important parameter indicating a minimum amphiphilic molecule concentration to form stable micelles in aqueous media. The CMC of the Lec-OAc complex was determined using fluorescence spectroscopy with pyrene as a fluorophore probe [21]. Pyrene is insoluble in water but it has limited solubility in hydrophobic parts of amphiphilic molecules. Under CMC, pyrene has no solubility and does not show any emission peak. However, over CMC, while the amphiphilic molecule turns into micelle in water, pyrene gains solubility and shows three distinct emission peaks. The first and third peak intensities ratio of pyrene (I3/I1) is a significant characteristic of CMC. When the amphiphilic molecule concentration reaches a critical concentration, micelles form and a profound increase in the emission intensities ratio of pyrene (I3/I1) is observed. In this study, at different concentrations of Lec-OAc ionic complex, pyrene was excited at 343 nm and the peak intensities at 386 nm (I3) and 360 nm (I1) were determined. CMC of the ionic complex was determined from the concentration corresponding to the sharp increase in the intensity

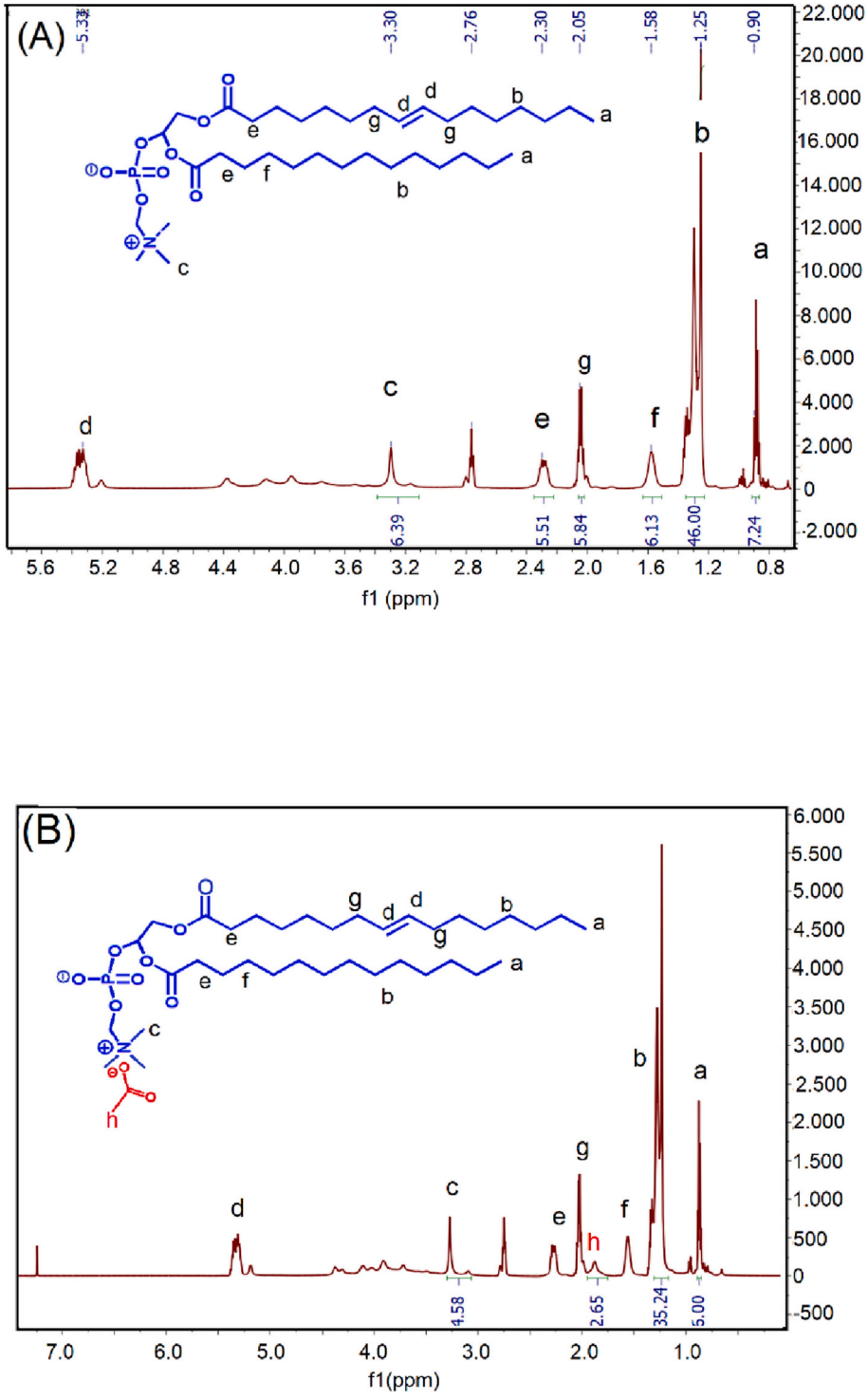

Fig. 3. ^{1}H NMR spectrum of lecithin (A); Lec-OAc complex (B).

ratio of (I3/I1) to be 1.047×10^{-4} M (Fig. 5) [20].

The CMC value of lecithin was reported to vary between 0.2×10^{-3} and 0.15×10^{-1} mM depending on the type of lecithin utilized (*i.e.*, egg yolk, soy lecithin, *etc.*) [41,42]. Thus, the calculated CMC value for Lec-OAc was quite favorable compared to the literature. Generally, as chain length (alkyl group) increases, the CMC decreases, and the ability to form micelles rises. It is notable that the lower CMC value of the Lec-OAc complex than soy-lecithin was considered to be the result of neutralization of the positive charges with OAc^{-}, which is another proof of the formation of stable Lec-OAc LNPs [43].

3.5. Particle size and zeta potential analyses of the synthesized LNPs

Particle size and zeta potential of Lec-OAc LNPs, QIn-Lec-OAc, Cur-Lec-OAc, and NPs indicated that Cur-loaded LNPs have a smaller average particle size than empty Lec-OAc LNPs. The average particle size of Cur-loaded LNPs decreased from 329 to 160 nm. This evidence demonstrated that Cur and Lec have strong molecular interactions with each other and the lipidic tile of lecithin is in the core. Thus, it could be hypothesized that the produced core structure of the LNPs gains density by Cur loading. After coating with QIn, the average particle size of NP

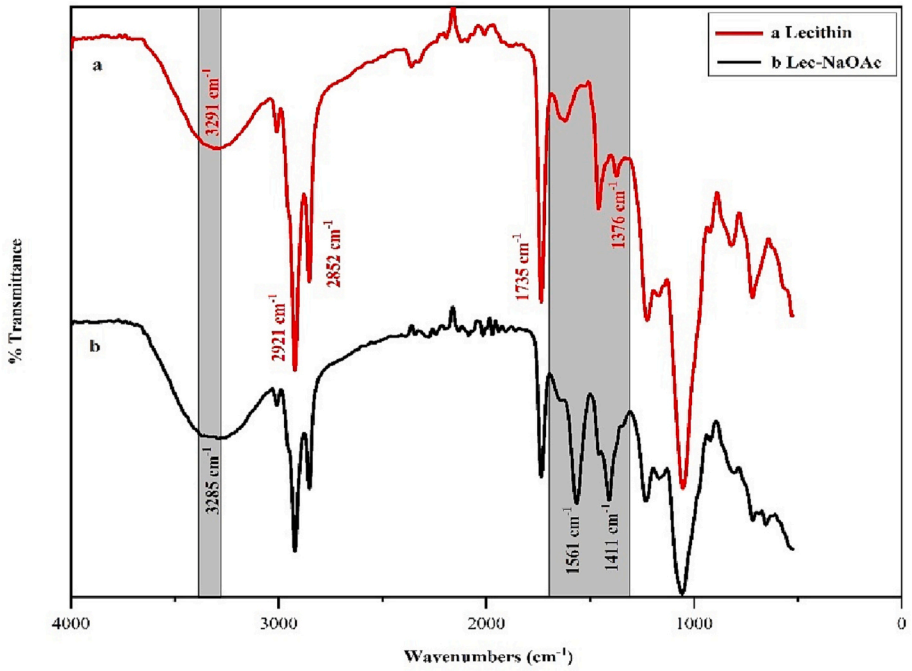

Fig. 4. The FTIR spectra of (a) soy lecithin and (b) Lec-OAc.

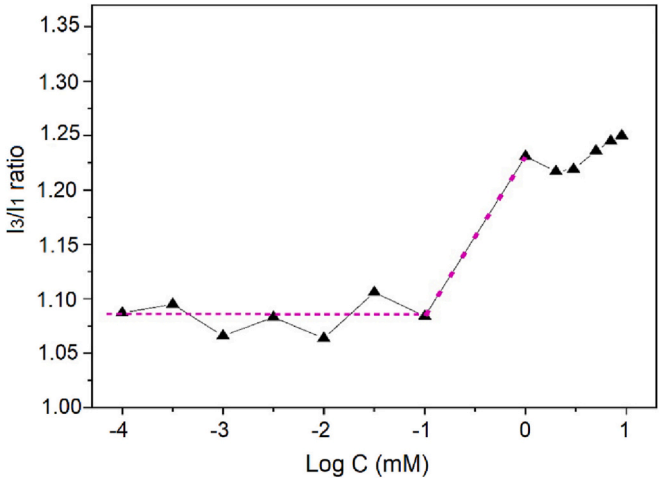

Fig. 5. The variation of the intensity ratio of pyrene emission peaks (I_3/I_1) with log concentration (Log C).

did not show any significant change compared to Lec-OAc. However, by loading Cur to the Lec-OAc-QIn coated particles, an increase in particle sizes observed, which could be related to the incorporation of Cur and the shell layer formed by QIn [44,45].

Zeta potential values of the samples changed from −26 to −5.38 mV (Table 1) with the coating of LNPs with QIn, indicating the success of the coating process. Despite the expected positive charges in the outer shell, the surface charge of samples had a slight negative zeta potential, which provided the formulation with good colloidal stability, caused by the repulsion of the particles in aqueous system. Although the incorporation of curcumin with QIn-LNP did not significantly change the zeta potential of LNPs, paclitaxel caused an increase in this parameter, indicating the settlement of paclitaxel in the QIn shell of the LNPs. Moreover, the increase in the size of LNPs by loading paclitaxel confirmed this hypothesis.

Table 1
Particle size and zeta analysis of complex, Cur-loaded complexes, and CurPtx-QIn-Lec-OAc NPs.

Sample name	Size distribution (nm) by:				Zeta value (mV):
	Number	Volume	Intensity	PDI	
Lec-OAc (LNPs)	329	351	365	0.672	−26
0.5 mg Cur loaded	160	178	173	0.724	−18.3
1.0 mg Cur loaded	133	157	150	0.623	−16.1
2.0 mg Cur loaded	167	178	171	0.387	−18.6
QIn-Lec-OAc	398	398	396	0.598	−5.38
0.5 mg Cur loaded	675	734	708	0.458	−6.68
1.0 mg Cur loaded	447	455	454	0.680	−6.91
2.0 mg Cur loaded	553	562	557	0.555	−8.50
Cur-Ptx loaded QIn-LNPs					
0.25 mg Cur + 0.25 mg Ptx	394	396	393	1	−0.40
0.50 mg Cur + 0.50 mg Ptx	584	593	585	0.7	−13.3
1.00 mg Cur + 1.00 mg Ptx	514	534	523	1	−18.0

3.6. DSC analysis

Differential scanning calorimetry (DSC) is a powerful thermo-analytical technique effectively used for measuring the amount of energy absorbed or released in the course of thermal transition of materials as a function of time and temperature [46]. In DSC thermograms, the peak areas and their corresponding temperature values provide valuable information on the morphology of materials.

The DSC curves of Cur, Ptx, and Cur-Ptx loaded QIn-Lec-OAc LNPs with different concentrations are shown in Fig. 6. Ptx and Cur are crystalline organic compounds with melting points of 219 °C and 178 °C, respectively, which are due to the crystalline structure of free Cur and Ptx. However, these characteristic peaks disappeared by incorporating Cur and Ptx into Lec-OAc-QIn LNPs (Fig. 6c, d, and e), suggesting that the drug materials entirely dissolved into the lipidic core of the LNPs. It could also be concluded that the Cur and Ptx molecules disturbed their crystalline domains and become amorphous in the core. The conversion

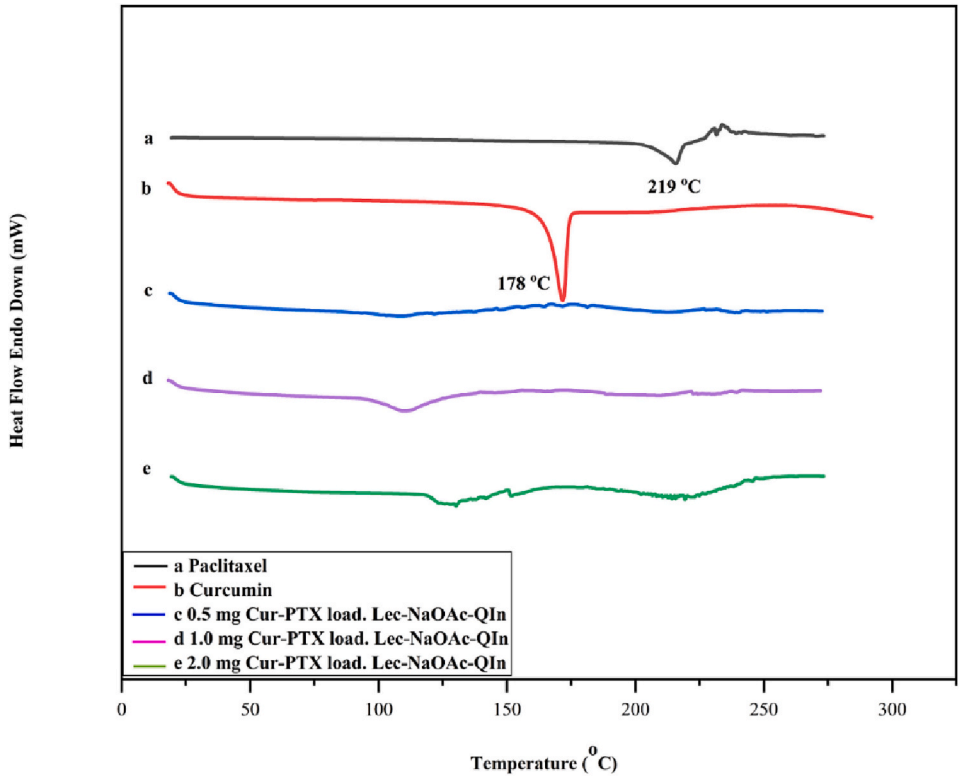

Fig. 6. DSC curves of (a) Ptx, (b) Cur, (c) 0.25 mg Cur and 0.25 mg Ptx, (d) 0.5 mg Cur and 0.5 mg Ptx, and (e) 1.0 mg Cur loaded and 1.0 mg Ptx loaded Lec-OAc-QIn.

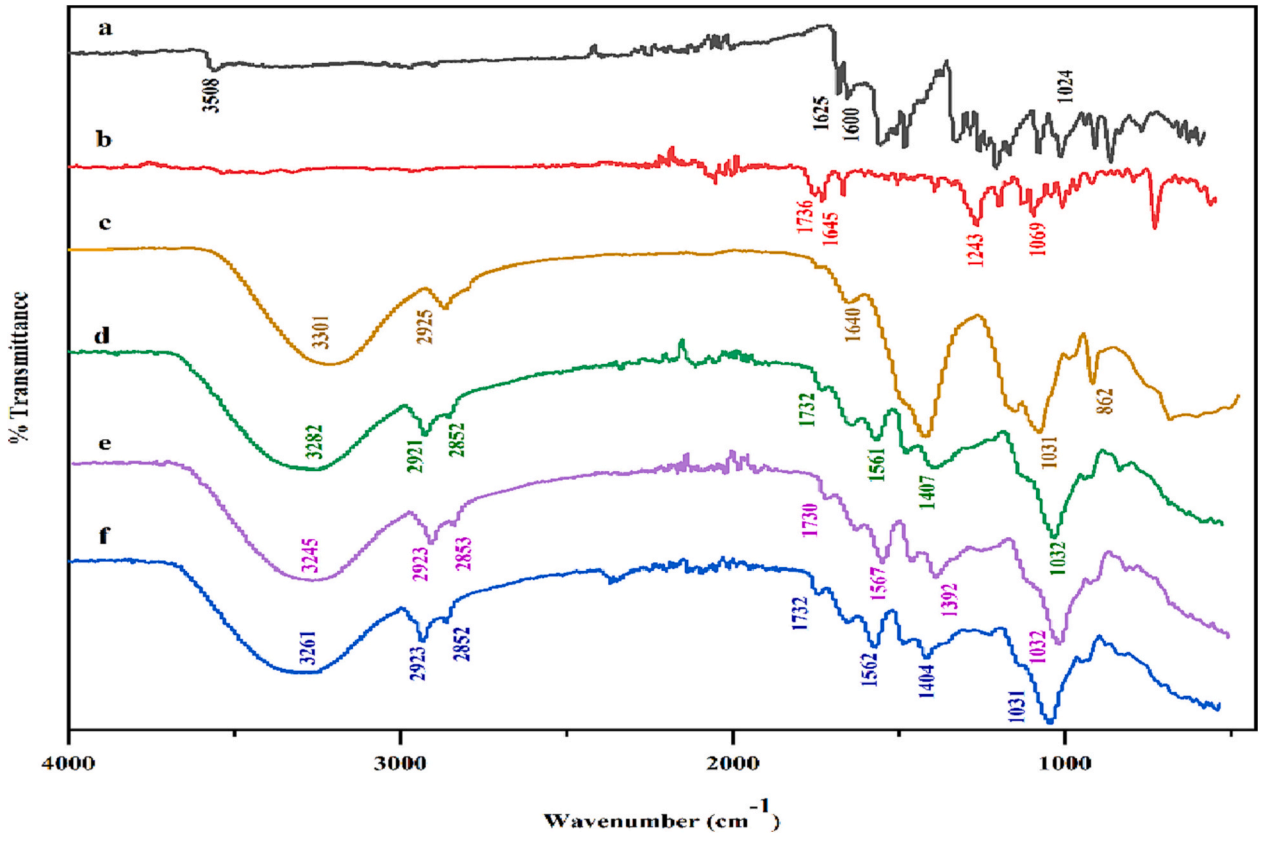

Fig. 7. The FTIR spectra of (a) Cur, (b) Ptx, (c) Lec-OAc-QIn (blank), (d) 0.5 mg cur and Ptx loaded Lec-OAc-QIn, (e) 1.0 mg cur and Ptx loaded Lec-OAc-QIn and (f) 2.0 mg cur and Ptx loaded Lec-OAc-QIn.

from a crystalline structure to an amorphous state enhances drug saturation and solubility [25,47]. Previously, it was shown that in the DSC thermogram of inulin, the endothermic peaks between 110 and 140 °C are due to water elimination and inulin melting peak, respectively [48]. With the increasing the amounts of Cur and Ptx, these two peaks shifted to higher temperatures, confirming the incorporation of drug molecules with inulin. Interaction of drug molecules with inulin makes it difficult for water molecules to evaporate by exposure to heat. They also cover the surrounding of inulin and allow it to melt at a higher temperature.

3.7. FTIR characterization

In the spectrum of Cur (Fig. 7a), the peaks at 3508 cm^{-1} corresponded to the stretching vibrations of the O—H and 1625 cm^{-1} was attributed to the C═C frequencies. The C—O—C band was observed at 1024 cm^{-1}. The spectrum of Ptx consisted of C═O stretching of paclitaxel at 1736 cm^{-1}, the characteristic C—C stretching at 1645 cm^{-1}, C—N stretching at 1243 cm^{-1}, and C—O stretching at 1069 cm^{-1} (Fig. 7b) [49]. In the spectrum of QIn-coated Lec-OAc (Fig. 7c), the peak at 3301 cm^{-1} was assigned to the O—H group. The peaks at 2925 cm^{-1} and the shoulder at 2851 cm^{-1} were attributed to C—H bonds in the fatty acid structure. These two peaks were identical for the total 0.5 mg, 1.0 mg, and 2.0 mg Cur and Ptx loaded QIn LNPs (with slight shifts in wavenumber). Moreover, the peak at 3301 cm^{-1}, assigned to the O—H group of curcumin disappeared indicating a successful encapsulation. The peak at 1031 cm^{-1} was attributed to stretching frequency of C—O—C of In. The presence of this peak (with a slight shift) in all CurPtx-QIn-LNP formulations indicated the presence of inulin in the outer shell of the synthesized NPs. In the spectrum of 0.5 mg Cur and Ptx loaded QIn coated LNPs (Fig. 7d), the band at 1737 cm^{-1} is due to the

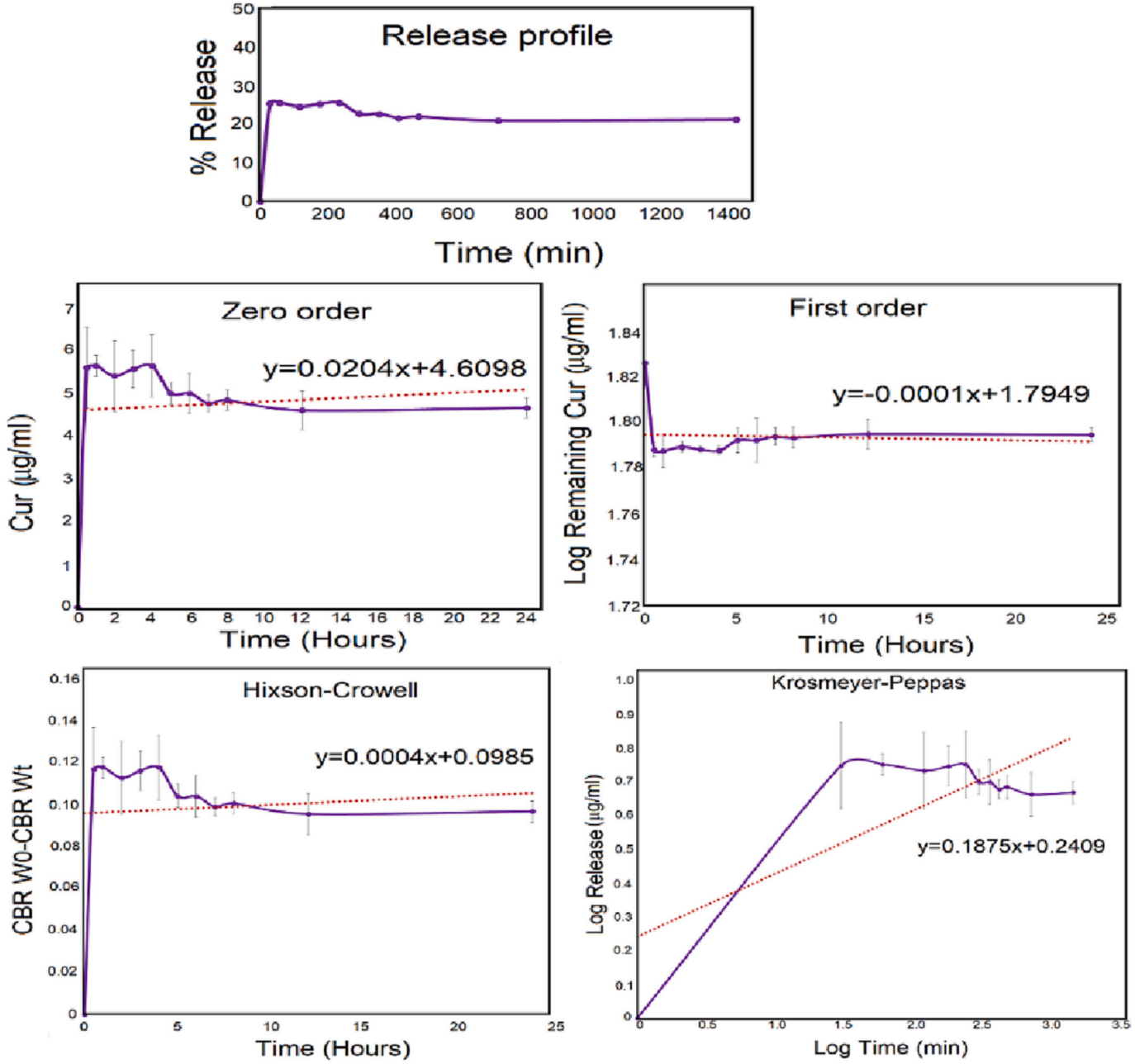

Fig. 8. Release profile of the QIn-LNP containing 2 mg Cur, R^2 values are: zero order: 0.0078, Hixson-Crowell: 0.0078, First order: 0.0065, and Korsmeyer-Peppas: 0.557.

–C═O moieties in Lec-OAc, which shifted to a higher wavenumber due to the incorporation of the drug molecules with these functional groups [50]. Furthermore, the C—O—C band became stronger after the drug loading, resulting from inulin and drug interaction (Fig. 7c). Moreover, the O—H group peak of blank LNPs at 3301 cm^{-1} shifted to lower frequencies for drug-loaded LNPs, confirming strong electrostatic interactions between the phenolic moiety of Cur and polymeric LNPs [51,52]. Along with all these evidences, the FTIR peaks of Ptx between 1730 cm^{-1} and 2400 cm^{-1} were observed in all CurPtx-QIn-LNP formulations. Considering that the FTIR spectrum of free QIn-coated LNPs showed no peak in this region, it could be concluded that some paclitaxel molecules incorporated with the outer Inulin shell of NP, which confirms our observations in DLS and DSC assays.

3.8. The Cur and Cur-PTX release profiles from QIn-LNPs and their release mechanisms

Drug release profiles of 2 mg Cur-loaded QIn-LNPs are shown in Fig. 8. The drug release study was applied for 24 h. The cumulative release of Cur increased as a function of time. The Cur, a highly hydrophobic drug, showed 25.63 % release at the end of 24 h. The cumulative release took place gradually. This slow release may occur due to the amorphization of some crystalline sections of the Cur and the inulin polymer.

In a previous study, a similar release profile of Cur was reported by Chehardoli et al. [53]. They prepared Inulin-Grafted Stearate-based polymeric NPs, and betamethasone was used as a drug against rheumatoid arthritis. According to their study, owing to the molecular attractions between inulin-grafted stearate NPs and hydrophobic drugs (betamethasone), the core structure acted as a host. Thus, a slow drug release was observed [53]. Then, the release kinetics of 2 mg of Cur from QIn-coated NPs was studied using models including zero order, Hixson-Crowell, first order, and Korsmeyer-Peppas (Fig. 8).

The release kinetics studies showed that the Korsmeyer-Peppas model with the highest correlation coefficient ($R^2 = 0.557$) is the best-fitted mathematical model for the release of Curcumin. An "$R^{2"}$ value

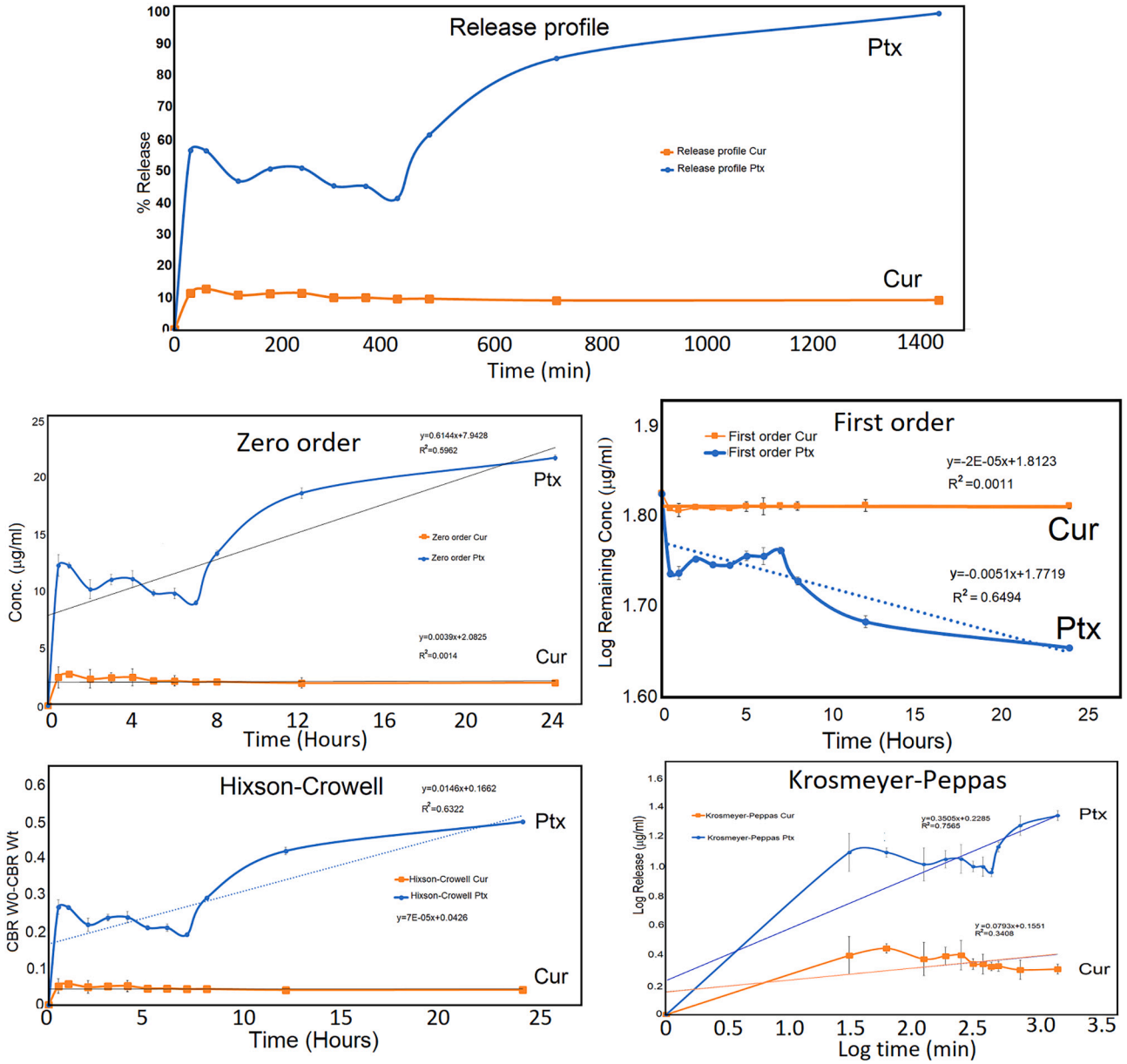

Fig. 9. Release profile of the QIn-LNP containing 1 mg Cur and 1 mg Ptx, R^2 values for Cur are: zero order: 0.0014, Hixson-Crowell: 0.0012, first order: 0.0011, and Korsmeyer-Peppas: 0.34, R^2 values for Ptx are: zero order: 0.59, Hixson-Crowell: 0.63, first order: 0.65, and Korsmeyer-Peppas: 0.76.

<0.82 was valid for the "Fickian Diffusion". This observation demonstrated that the release of Cur occurred *via* molecular diffusion through a polymeric matrix [54–56]. Fig. 9 shows the release profile of 1.0 mg Ptx and 1.0 mg Cur loaded to the QIn-LNP NPs.

Although the incorporation of Ptx into the drug delivery system caused the settlement of the drug in the outer shell of LNPs (as shown in DLS, DSC, and FTIR assays), interestingly, its release was not so fast. Furthermore, the release of Cur was slowed down significantly while it is associated with Ptx. It could be concluded that Ptx not only integrated with the LNP constituents but also with Cur molecules, which caused a decrease in the release period. Korsmeyer-Peppas, with "R^{2}" values higher than the other mathematical models, was the preferred model for both paclitaxel and Curcumin. This evidence shows that Ptx loading does not cause any change in the release mechanism of Cur, and the release occurs *via* diffusion for both drug molecules.

3.9. SEM and TEM

SEM images of blank Lec-OAc LNPs and Cur-loaded QIn-coated LNPs showed that the LNPs had spherical shapes and mostly homogenous particle sizes. However, some portions of the LNPs were embedded into the lipidic matrix and agglomerated, which was assumed to occur due to the collisions of the molecules during the drying stage. Fig. 10b–c shows TEM images of Cur-loaded and QIn coated LNPs, which demonstrate a very homogenous spherical form, evidently covered with QIn. The Cur-loaded core appeared darker in the TEM images, while a corona layer formed by QIn appeared relatively lighter which is ideal for drug delivery systems.

3.10. In vitro cytotoxicity assay results

CurPtx-QIn-LNP showed weaker cytotoxicity than both CurPtx-LNP and Ptx (Fig. 11). However, as the time progressed, the toxicity of CurPtx-QIn-LNP began to show a stronger effect than the uncoated formulation (CurPtx-LNP) and even the free Ptx, which was attributed to the importance of QIn a glucose-like macro-molecule in the cell internalization of the synthesized NPs.

The cytotoxic activities of Cur and Ptx are higher than Cur-Ptx-LNP and Cur-Ptx-QIn-LNP. This is due to the period which is needed for the cell internalization of NDDS. However, at the end of 72 h, Cur-Ptx-QIn-LNP shows a stronger cytotoxic activity than Cur. The cytotoxic activity of Cur-Ptx-QIn-LNPs was found not to be different in a statistically significant manner than that of Ptx. Considering the fast release of Ptx from NP, this insignificant difference can become meaningful. However, despite the very slow release of Cur from NP (10 % release at 24 h) the cytotoxicity of Cur-Ptx-QIn-LNP increases with time. This fact shows that the cytotoxicity of NDDS is due to its successful cell internalization and the release of the drug inside of the cell by enzymatic reactions. The very weak cytotoxic activity of bare Cur at the end of 72 h confirms this fact. Furthermore, the cells treated with QIn-LNP show a very high cell survival which confirms the cytotoxic activity of Cur-Ptx-QIn-LNP is due to its successful cell internalization and the release of the drugs inside of the cells.

Mutlu et al. [57] developed quaternized *Halomonas* levan-coated lecithin-based NPs for efficiently delivering Ptx to human lung A549 cancer cells. They suggested that the coating process was effective due to the zeta potential of the lecithin-based NPs changing from −75 mV to −0.85 mV after the coating of the quaternized *Halomonas* levan. Furthermore, they discovered that the quaternized *Halomonas* levan

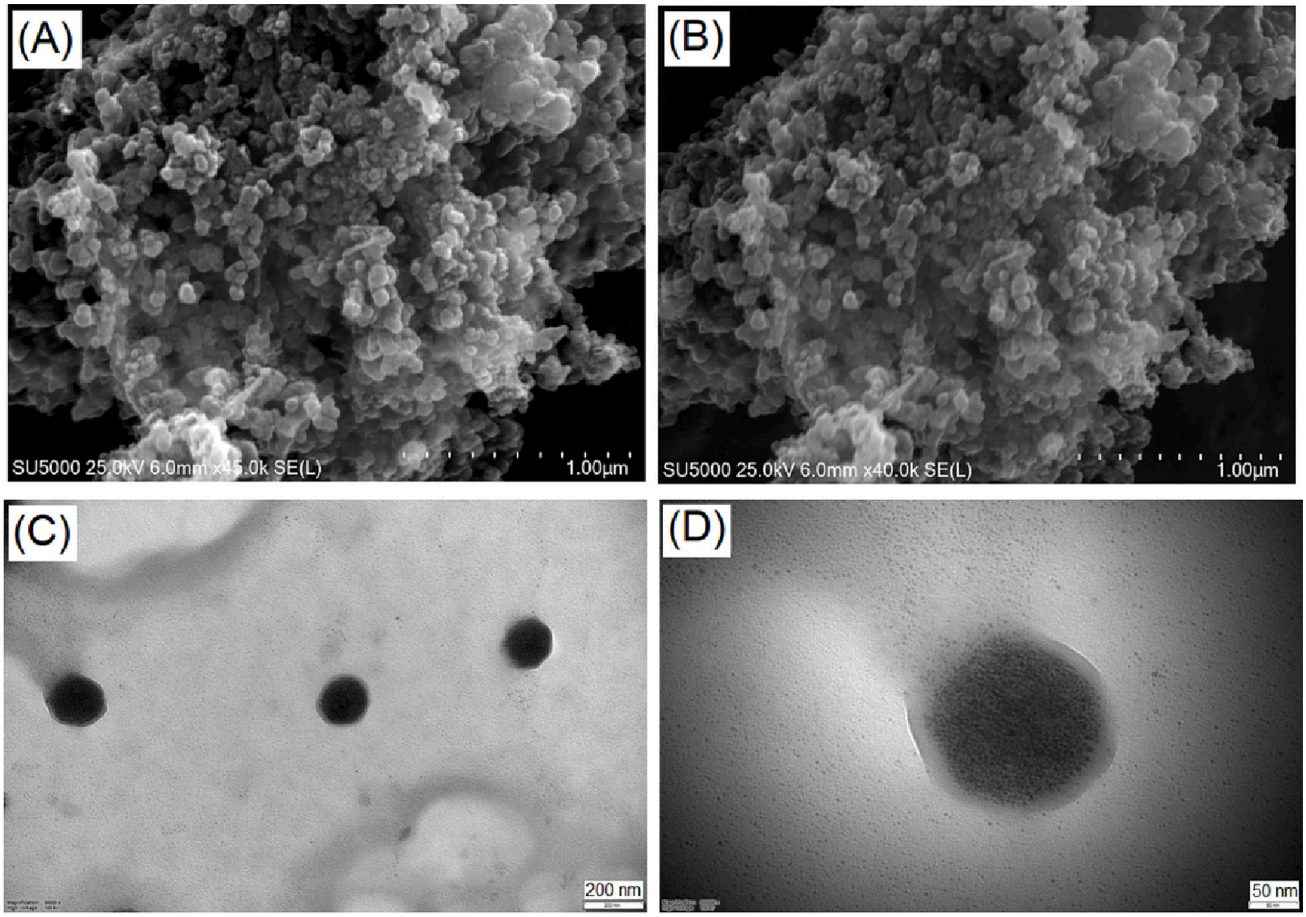

Fig. 10. SEM and TEM images of NPs at different magnifications: a) 45,000, b) 40,000, c) 150,000 and d) 300,000.

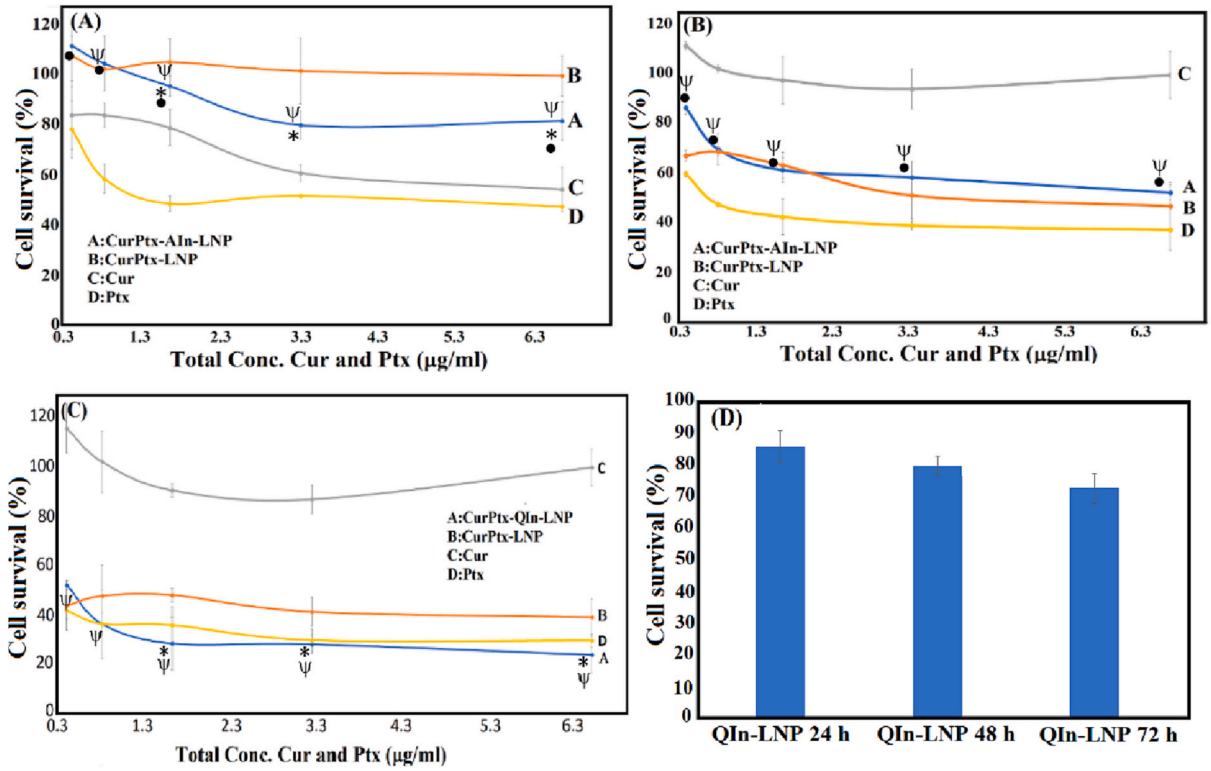

Fig. 11. *In vitro* cytotoxicity of CurPtx-QIn-LNP, CurPtx-LNP, Cur, and Ptx in A) 24 h, B) 48 h, C)72 h on MDA-MB-231, and D) of bare QIn-LNP at 24, 48, and 72 h. Efficacy comparison was done between the cytotoxicity of Cur-Ptx-QIn-LNPs and other groups (namely bare Cur, Ptx, CurPtx-LNPs) were analyzed using ANOVA ($p < 0.05$). *: significantly different cytotoxic activity between Cur-Ptx-QIn-LNP and CurPtx-LNP. •: significantly different cytotoxic activity between Cur-Ptx-QIn-LNP and Ptx. ψ: significantly different cytotoxic activity between Cur-Ptx-QIn-LNP and Cur.

shell prevents fast release of PTX and offers a long period release of PTX. In current study similar results are obtained using QIn as coating material. Similar to the results obtained in our current study, the toxicity of Ptx carrying Levan coated NPs increased with time and their anticancer efficacy outbalanced the effect of other groups at the end of 72 h. However, QIn shows superior toxic profile compared to that of Levan, because the Levan coated NPs have caused 60 % cell death on A549 lung cancer cells, while QIn coated NPs caused only 25 % cell death at the end of 72 h. Therefore, they concluded that quaternized *Halomonas* levan-coated lipid NPs have an excellent therapeutic effect [57].

4. Conclusion

To our best knowledge, quaternized inulin (QIn) has not been used as a surface coating material for NDDSs in the literature. This research aimed to investigate the possibility of increasing the efficacy of Lecithin-based NDDS in terms of elucidating physicochemical properties and *in-vitro* efficacy through surface coating with QIn. Furthermore, drug release profiles and release kinetics were investigated to understand the effects of QIn on the biological effects of the uploaded drug molecules (Cur and Ptx).

The quaternized inulin (QIn) was successfully produced and used for the surface coating of the LNPs. The coated LNPs showed fair zeta potential values in cell internalization and *ex-vivo* stability. QIn-coated LNPs exhibited spherical core-shell structures in TEM images. The FTIR and DSC results showed that Cur was incorporated into the lipid core of LNPs, while Ptx was partially settled on the QIn-shell. However, the partial settlement of Ptx at the outer shell of the LNPs neither affected the release rate nor changed the release mechanism of CurPtx-QIn-LNPs. This was attributed to the interaction of Ptx with QIn on the shell, and with Cur and lecithin in the core. The CMC value of the Lec-OAc complex was determined to be 1.047 × 10–4 M, which is lower than the CMC value of lecithin alone. The cumulative release of Cur was found to be 25.63 %, due to the interactions between the components of the NDDS and the drug molecules. Korsmeyer-Peppas and the diffusion of drug molecules from NDDS exhibited the best model in our LNPs for drug release kinetics. Since the erosion of the components of NDDS in blood circulation is not a favorable property, the obtained results can be counted as an advantage of the newly synthesized LNPs as cancer therapy agents. Cytotoxicity assays confirmed the role of QIn in the internalization of CurPtx-QIn-LNPs by enhancing the efficacy of drug molecules over time. Although no statistically significant different results were obtained from the cytotoxic activity of bare Ptx and Cur-Ptx-QIn-LNPs at the end of 72 h the cytotoxicity of Cur-Ptx-QIn-LNPs was found to be stronger than both bare Ptx and Cur molecules. The equal cytotoxic activity of Ptx and Cur-Ptx-QIn-LNPs could be attributed to the very fast release of Ptx from Cur-Ptx-QIn-LNPs (100 % release within 24 h). However, Cur shows a very slow release from Cur-Ptx-QIn-LNPs (only 10 % at the end of 24 h) and the increase in the cytotoxicity of Cur-Ptx-QIn-LNPs shows the internalization of particles to the cells and efficacy of Cur inside of the cell.

CRediT authorship contribution statement

Ozgun Vatansever: Synthesis, sample preparation, writing draft.

Fatemeh Bahadori: Statistical analyses/writing/cell studies/original draft.

Seyma Bulut: Cell studies.

Mehmet Sayip Eroglu: Corresponding author/Conceptualization/Supervision/Writing/Revision/Funding acquisition.

Declaration of competing interest

The authors declare that they have no known competing financial

interests or personal relationships that could have appeared to influence the work reported in this paper.

Data availability

Data will be made available on request.

Acknowledgement

This work was supported by Marmara University project numbers FEN-C-DRP130319-0068 and FEN-E-130515-0175.

References

[1] R. Kotecha, A. Takami, J.L. Espinoza, Dietary phytochemicals and cancer chemoprevention: a review of the clinical evidence, Oncotarget 7 (32) (2016) 52517–52529.
[2] W. Wang, T. Chen, H. Xu, B. Ren, X. Cheng, R. Qi, H. Liu, Y. Wang, L. Yan, S. Chen, Q. Yang, C. Chen, Curcumin-loaded solid lipid nanoparticles enhanced anticancer efficiency in breast cancer, Molecules 23 (7) (2018).
[3] L. Pathak, A. Kanwal, Y. Agrawal, Curcumin loaded self assembled lipid-biopolymer nanoparticles for functional food applications, J. Food Sci. Technol. 52 (10) (2015) 6143–6156.
[4] Y. Chen, Y. Lu, R.J. Lee, G. Xiang, Nano encapsulated curcumin: and its potential for biomedical applications, Int. J. Nanomedicine 15 (2020) 3099–3120.
[5] C. Righeschi, M.C. Bergonzi, B. Isacchi, C. Bazzicalupi, P. Gratteri, A.R. Bilia, Enhanced curcumin permeability by SLN formulation: the PAMPA approach, LWT Food Sci. Technol. 66 (2016) 475–483.
[6] H. Yavarpour-Bali, M. Ghasemi-Kasman, M. Pirzadeh, Curcumin-loaded nanoparticles: a novel therapeutic strategy in treatment of central nervous system disorders, Int. J. Nanomedicine 14 (2019) 4449–4460.
[7] S. Madderla, P.T. Sundari, Formulation and evaluation of curcumin loaded solid lipid nanoparticles by employing Cutina® Hr and Tween 80, Int.J.Res.Anal.Rev. 5 (4) (2018) 812–819.
[8] S.A. Adefegha, A. Salawi, A. Bumrungpert, S. Khorasani, S. Torkaman, M. Mozafari, E. Taghavi, Encapsulation of polyphenolic compounds for health promotion and disease prevention: challenges and opportunities, Nano Micro Biosyst. 1 (2) (2023) 1–12.
[9] P. Ma, R.J. Mumper, Paclitaxel nano-delivery systems: a comprehensive review, J. Nanomed. Nanotechnol. 4 (2) (2013), 1000164.
[10] J. Fang, W. Islam, H. Maeda, Exploiting the dynamics of the EPR effect and strategies to improve the therapeutic effects of nanomedicines by using EPR effect enhancers, Adv. Drug Deliv. Rev. 157 (2020) 142–160.
[11] F. Li, G. Sethi, Targeting transcription factor NF-κB to overcome chemoresistance and radioresistance in cancer therapy, Biochim. Biophys. Acta, Rev. Cancer 1805 (2) (2010) 167–180.
[12] L.-L. Yu, J.-G. Wu, N. Dai, H.-G. Yu, J.-M. Si, Curcumin reverses chemoresistance of human gastric cancer cells by downregulating the NF-κB transcription factor, Oncol. Rep. 26 (5) (2011) 1197–1203.
[13] T.M. Allen, P.R. Cullis, Drug delivery systems: entering the mainstream, Science 303 (5665) (2004) 1818–1822.
[14] M. Singh, R. Mishra, S. Dubey, P. Roy, R.P. Singh, Surface grafted core-shell chitosan-modified solid lipid nanoparticles: characterization and application in hydrophobic drug delivery, in: D.W. Piyawattanametha (Ed.), Proceedings of the 14th Annual IEEE International Conference on Nano/Micro Engineered and Molecular Systems, Bangkok, Thailand, 2019, pp. 529–533.
[15] F. Afinjuomo, S. Abdella, S.H. Youssef, Y. Song, S. Garg, Inulin and its application in drug delivery, Pharmaceuticals (Basel) 14 (9) (2021).
[16] X.-M. Chen, G.-Y. Tian, Structural elucidation and antitumor activity of a fructan from Cyathula officinalis Kuan, Carbohydr. Res. 338 (11) (2003) 1235–1241.
[17] D. Lombardo, P. Calandra, M. Teresa Caccamo, S. Magazù, M. Alekseyevich Kiselev, Colloidal stability of liposomes, AIMSMater. Sci. 6 (2) (2019) 200–213.
[18] M.R. Islam Shishir, N. Karim, V. Gowd, X. Zheng, W. Chen, Liposomal delivery of natural product: a promising approach in health research, Trends Food Sci. Technol. 85 (2019) 177–200.
[19] E. Mutlu, in: A Novel Design of Levan Based Tumour Targeting Nano-scale Micelles, Chemical Engineering, Marmara University, Istanbul, 2014, pp. 1–125.
[20] R. Gruškienė, R. Deveikytė, R. Makuška, Quaternization of chitosan and partial destruction of the quaternized derivatives making them suitable for electrospinning, Chemija 24 (4) (2013) 325–334.
[21] M.A. Karimi, M.A. Mozaheb, A. Hatefi-Mehrjardi, H. Tavallali, A.M. Attaran, R. Shamsi, A new simple method for determining the critical micelle concentration of surfactants using surface plasmon resonance of silver nanoparticles, J.Anal.Sci. Technol. 6 (1) (2015).
[22] I. Badea, D. Ciutaru, L. Lazar, D. Nicolescu, A. Tudose, Rapid HPLC method for the determination of paclitaxel in pharmaceutical forms without separation, J. Pharm. Biomed. Anal. 34 (3) (2004) 501–507.
[23] F. Bahadori, B.S. Akinan, S. Akyıl, M.S. Eroğlu, Synthesis and engineering of sodium alginate/inulin core-shell nano-hydrogels for controlled-release oral delivery of 5-ASA, Org.Commun. 12 (3) (2019) 132–142.
[24] J.R.C. Reddy, B.V.S.K. Rao, M.S. Karuna, K.V.S.N. Raju, A.V.R. Krishna, R.B. N. Prasad, Lipase-mediated preparation of epoxy lecithin and its evaluation as plasticizer in polyester laminates, J. Appl. Polym. Sci. 127 (4) (2013) 2945–2951.
[25] E.C. Mutlu, M.S. Bostan, F. Bahadori, A. Kocyigit, E.T. Oner, M.S. Eroglu, Lecithin-acrylamido-2-methylpropane sulfonate based crosslinked phospholipid nanoparticles as drug carrier, J. Appl. Polym. Sci. 133 (42) (2016).
[26] R. Walesa, T. Ptak, D. Siodlak, T. Kupka, M.A. Broda, Experimental and theoretical NMR studies of interaction between phenylalanine derivative and egg yolk lecithin, Magn. Reson. Chem. 52 (6) (2014) 298–305.
[27] C. Prasad, E. Bhatia, R. Banerjee, Curcumin encapsulated lecithin nanoemulsions: an oral platform for ultrasound mediated spatiotemporal delivery of curcumin to the tumor, Sci. Rep. 10 (1) (2020) 8587.
[28] A. Singh, N. Thotakura, R. Kumar, B. Singh, G. Sharma, O.P. Katare, K. Raza, PLGA-soya lecithin based micelles for enhanced delivery of methotrexate: cellular uptake, cytotoxic and pharmacokinetic evidences, Int. J. Biol. Macromol. 95 (2017) 750–756.
[29] R.P. D'Amelia, M.W. Kimura, W.F. Nirode, Application of quantitative proton nuclear magnetic resonance spectroscopy for the compositional analysis of short-chain fatty acid ethyl ester mixtures, World J.Chem.Educ. 9 (1) (2020) 8–13.
[30] M.E. Azenha, H.D. Burrows, S.M. Fonseca, M.L. Ramos, J. Rovisco, J.S. de Melo, A. J.F.N. Sobral, K. Kogej, Luminescence from cerium(iii) acetate complexes in aqueous solution: considerations on the nature of carboxylate binding to trivalent lanthanides, New J. Chem. 32 (9) (2008).
[31] S.Y. Ghan, L.F. Siow, C.P. Tan, K.W. Cheong, Y.Y. Thoo, Influence of soya lecithin, sorbitan and glyceryl monostearate on physicochemical properties of organogels, Food Biophys. 15 (3) (2020) 386–395.
[32] R. Tantipolphan, T. Rades, A.J. McQuillan, N.J. Medlicott, Adsorption of bovine serum albumin (BSA) onto lecithin studied by attenuated total reflectance Fourier transform infrared (ATR-FTIR) spectroscopy, Int. J. Pharm. 337 (1–2) (2007) 40–47.
[33] N. Meng, X. Chu, M.Q. Ge, M. Zhang, B. Sun, Y.-T. Su, N.-L. Zhou, Preparation and characterization of lecithin–heparin intercalated in montmorillonite nanocomposite, Appl. Clay Sci. 162 (2018) 454–460.
[34] S. Yang, L. Dai, C. Sun, Y. Gao, Characterization of curcumin loaded gliadin-lecithin composite nanoparticles fabricated by antisolvent precipitation in different blending sequences, Food Hydrocoll. 85 (2018) 185–194.
[35] R. Silva, L.R.S. Lara, J. López, Á. Andrade, J. Oliveira, J. Takahashi, H. Vieira, T. Matencio, H. Stumpf, R. Domingues, Preparation of magnetoliposomes with a green, low-cost, fast and scalable methodology and activity study against S. aureus and C. freundii bacterial strains, J. Braz. Chem. Soc. 29 (2018) 2636–2645.
[36] H.F. Abo-Hatab, N.G. Kandile, H.M. Salah, Eco-friendly multifunction petroleum additives: preparation,characterization and evaluation, Tribol. Ind. 40 (1) (2018) 129–138.
[37] W. Michal, D. Ewa, C. Tomasz, Lecithin-based wet chemical precipitation of hydroxyapatite nanoparticles, Colloid Polym. Sci. 293 (5) (2015) 1561–1568.
[38] M.J. Al-Kheetan, S.H. Ghaffar, O.A. Madyan, M.M. Rahman, Development of low absorption and high-resistant sodium acetate concrete for severe environmental conditions, Constr. Build. Mater. 230 (2020).
[39] Y. Cui, Y. Zhu, R. Dai, Z. Shan, J. Yi, H. Chen, The solubility and interactions of gelatin in "water-in-sodium acetate trihydrate/urea-DES" system, Colloids Surf. A Physicochem. Eng. Asp. 625 (2021).
[40] C. Iacovita, R. Stiufiuc, T. Radu, A. Florea, G. Stiufiuc, A. Dutu, S. Mican, R. Tetean, C.M. Lucaciu, Polyethylene glycol-mediated synthesis of cubic iron oxide nanoparticles with high heating power, Nanoscale Res. Lett. 10 (1) (2015) 391.
[41] N.G. Eskandar, S. Simovic, C.A. Prestidge, Interactions of hydrophilic silica nanoparticles and classical surfactants at non-polar oil–water interface, J. Colloid Interface Sci. 358 (1) (2011) 217–225.
[42] R. Bhatta, H. Chandasana, Y. Chhonker, C. Rathi, D. Kumar, K. Mitra, P. Shukla, Mucoadhesive nanoparticles for prolonged ocular delivery of natamycin: in vitro and pharmacokinetics studies, Int. J. Pharm. 432 (1–2) (2012) 105–112.
[43] B. Brycki, A. Szulc, H. Koenig, I. Kowalczyk, T. Pospieszny, S. Górka, Effect of the alkyl chain length on micelle formation for bis(N-alkyl-N, N-dimethylethylammonium)ether dibromides, C. R. Chim. 22 (5) (2019) 386–392.
[44] A.M. Raja, S.Z. Muhammad, A.C. Liu, Self-assembled nanoparticles based on amphiphilic chitosan derivative and arginine for oral curcumin delivery, Int. J. Nanomedicine 11 (2016) 4397–4412.
[45] M. Hasan, G. Ben Messaoud, F. Michaux, A. Tamayol, C.J.F. Kahn, N. Belhaj, M. Linder, E. Arab-Tehrany, Chitosan-coated liposomes encapsulating curcumin: study of lipid–polysaccharide interactions and nanovesicle behavior, RSCAdv. 6 (51) (2016) 45290–45304.
[46] R.I.M. Almoselhy, Applications of differential scanning calorimetry (DSC) in oils and fats research.A review, Am. Res. J. Agric. 6 (1) (2020) 1–9.
[47] N. Tahir, A. Madni, A. Correia, M. Rehman, V. Balasubramanian, M.M. Khan, H. A. Santos, Lipid-polymer hybrid nanoparticles for controlled delivery of hydrophilic and lipophilic doxorubicin for breast cancer therapy, Int. J. Nanomedicine 14 (2019) 4961–4974.
[48] C. Blecker, J.-P. Chevalier, C. Fougnies, J.-C. Van Herck, C. Deroanne, M. Paquot, Characterisation of different inulin samples by DSC: influence of polymerisation degree on melting temperature, J. Therm. Anal. Calorim. 71 (1) (2003) 215–224.
[49] P.T. Ha, H.N. Nguyen, H.D. Do, Q.T. Phan, M.N.T. Thi, X.P. Nguyen, M.N.H. Thi, M.H. Le, L.T. Nguyen, T.Q. Bui, Targeted drug delivery nanosystems based on copolymer poly (lactide)-tocopheryl polyethylene glycol succinate for cancer treatment, Adv. Nat. Sci. Nanosci. Nanotechnol. 7 (1) (2016), 015001.
[50] F. Bahadori, Z. Eskandari, N. Ebrahimi, M.S. Bostan, M.S. Eroğlu, E.T. Oner, Development and optimization of a novel PLGA-Levan based drug delivery system

for curcumin, using a quality-by-design approach, Eur. J. Pharm. Sci. 138 (2019), 105037.
[51] Z. Zareie, F. Tabatabaei Yazdi, S.A. Mortazavi, Optimization of gamma-aminobutyric acid production in a model system containing soy protein and inulin by Lactobacillus brevis fermentation, J.Food Meas.Charact. 13 (4) (2019) 2626–2636.
[52] O. Sreekanth Reddy, M.C.S. Subha, T. Jithendra, C. Madhavi, K. Chowdoji Rao, Curcumin encapsulated dual cross linked sodium alginate/montmorillonite polymeric composite beads for controlled drug delivery, J. Pharm. Anal. 11 (2) (2021) 191–199.
[53] G. Chehardoli, P. Norouzian, F. Firozian, Inulin-grafted stearate (In-g-St) as the effective self-assembling polymeric micelle: synthesis and evaluation for the delivery of betamethasone, J. Nanomater. 2020 (2020) 1–8.
[54] T.K. Aniesrani, D.S. Delfiya, Evaluation of in vitro release pattern of curcumin loaded egg albumin nanoparticles prepared using acetone as desolvation agent, Curr. Trends Biotechnol. Pharm. 10 (2) (2016) 125–135.
[55] A.M. Craciun, M.L. Barhalescu, M. Agop, L. Ochiuz, Theoretical modeling of long-time drug release from nitrosalicyl-imine-chitosan hydrogels through multifractal logistic type laws, Comput. Math. Methods Med. 2019 (2019) 4091464.
[56] R.-D. Pavaloiu, Fawzia Sha'at, Cristina Hlevca, Mousa Sha'at, Gabriela Savoiu, Sibel Osman, Evaluation of drug release kinetics from polymeric nanoparticles loaded with poorly water-soluble APIs, Ovidius Univ. Ann. Chem. 32 (2) (2021) 132–136.
[57] E.C. Mutlu, F. Bahadori, M.S. Bostan, H.K. Sarilmiser, E. ToksoyOner, M.S. Eroğlu, Halomonas levan-coated phospholipid based nano-carrier for active targeting of A549 lung cancer cells, Eur. Polym. J. 144 (2021).